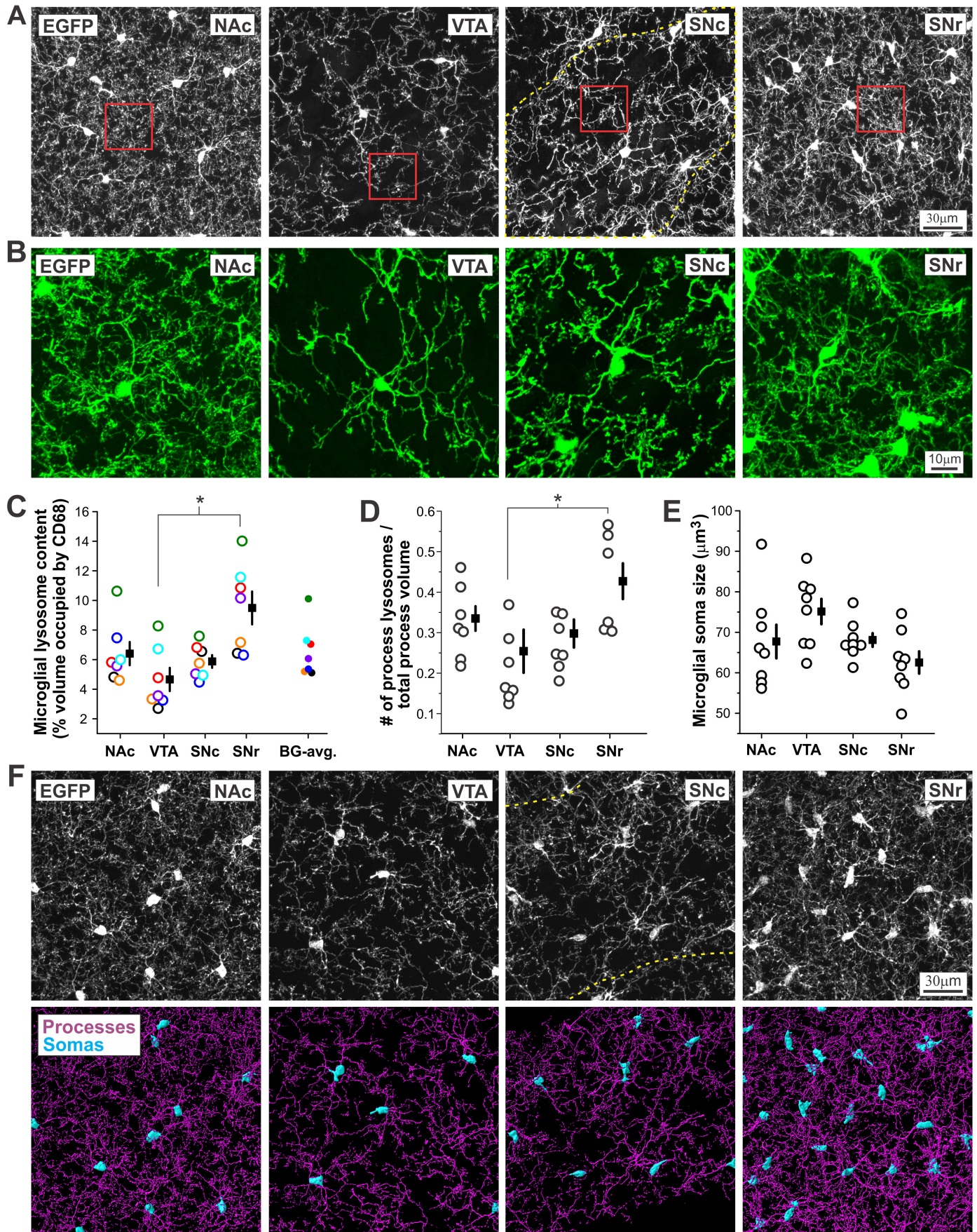
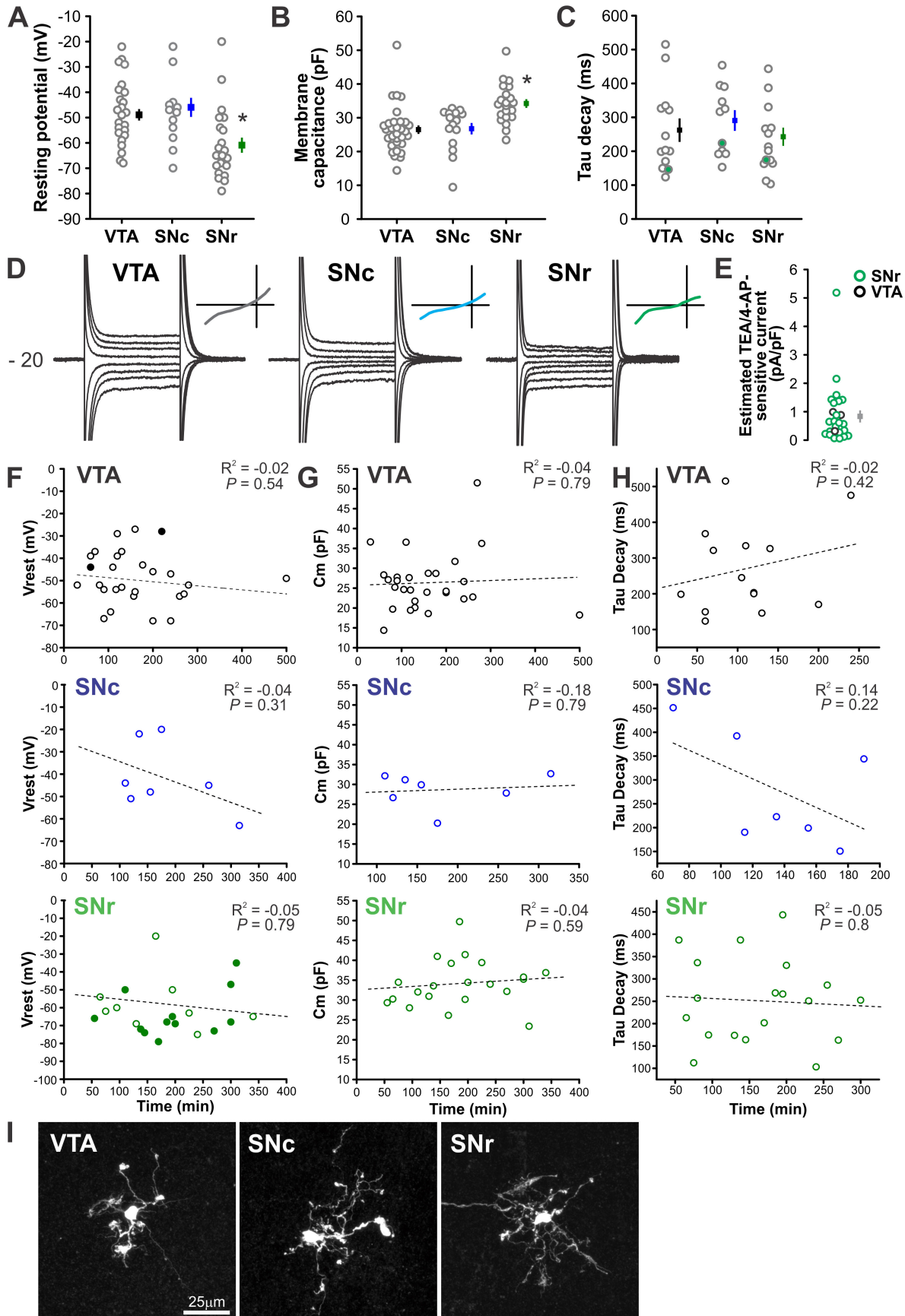


Figure S1. Related to Figures 2-3.



Supplementary Figure 1. Detailed morphological features and lysosome content of basal ganglia microglia. Related to Figures 2-3. **A** – immunostaining for EGFP in fields of view analyzed for microglial tissue coverage; *red boxes* indicate regions shown at higher magnification in *Fig. 2A*. *Dashed yellow line* indicates the boundaries of the SNc. **B** – EGFP immunostaining for individual microglial cells reconstructed in *Fig. 2C*. **C** – Lysosome content of BG microglia (% volume occupied by CD68). Data points from the same mouse are the same color across BG regions. *Filled circles at right* – represent average microglial lysosome content across all BG regions; used to compute normalized lysosome content shown in *Fig. 3B*. ANOVA $F(3,24) = 6.4$, $P = 0.025$; * $P = 0.004$ VTA vs. SNr. **D** – Number of lysosomes within microglial processes normalized to overall volume of microglial processes in that brain region. ANOVA $F(3,24) = 5.7$, $P = 0.004$; * $P = 0.005$ VTA vs. SNr. **E** – Size of microglial somas in each brain region as measured by 3D reconstruction shown in *F*. ANOVA $F(3,28) = 2.9$, $P = 0.052$ (n.s.). **F** – Representative images of microglia from each brain region (*top*, EGFP) and 3D reconstruction of cell somas and processes (*bottom*) illustrating the strategy used to calculate soma size and lysosomal abundance within somas and processes. *Dashed yellow line* indicates the boundaries of the SNc. N = 7-8 mice per region for all analyses.

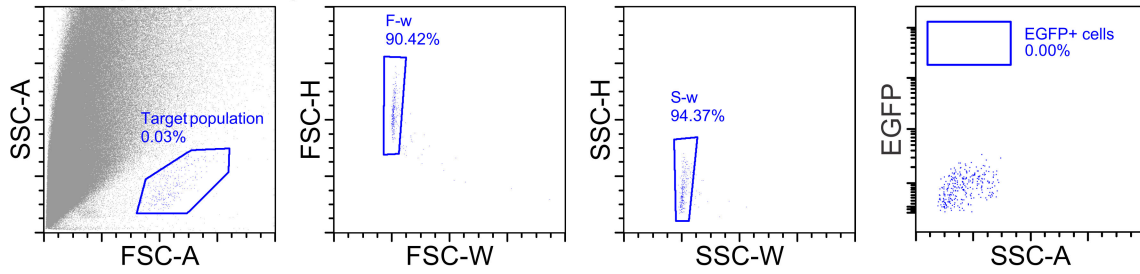
Figure S2. Related to Figure 4.



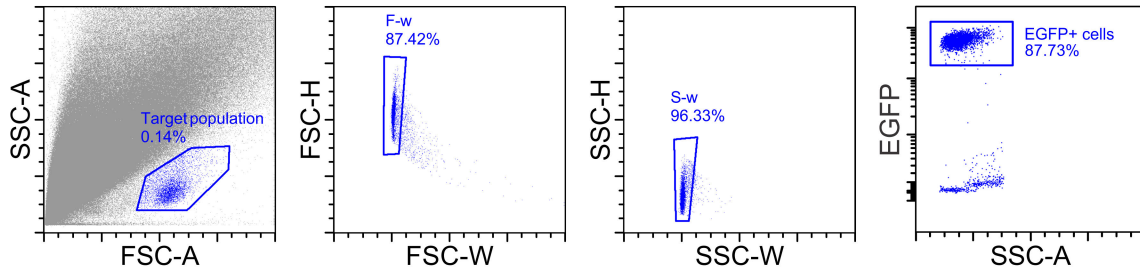
Supplementary Figure 2. Basic membrane properties of midbrain BG microglia; recorded membrane properties are not associated with reactive changes in microglia. Related to Figure 4. **A** – Resting membrane potential of midbrain BG microglia. ANOVA $F(2,64) = 7.0$, $P = 0.002$; * $P < 0.004$ SNr vs. VTA and SNr vs. SNc; VTA vs SNc = n.s., N = 14 - 31 cells total per region, 1-3 cells recorded from 8-15 different mice. **B** – Membrane capacitance of midbrain BG microglia. ANOVA $F(2,64) = 9.8$ * $P < 0.001$ SNr vs. VTA and SNr vs. SNc; VTA vs SNc = n.s., N = 15 - 31 cells total per region, 1-3 cells recorded from 8-15 different mice. **C** – Input resistance of midbrain BG microglia. ANOVA $F(2,36) = 0.52$, $P = 0.6$, N = 11 - 15 cells total per region, 1-3 cells recorded from 5-6 different mice. *Filled green circles* indicate tau decay values calculated from example cells shown in *Fig. 4A*. **D** – Responses of representative microglial cells shown in *Fig. 4B* when stepped to holding potentials from -120 mV to +30 mV from an initial holding potential of -20 mV. *Inset* shows resulting I-V relationship. **E** – Estimated magnitude of observed K_v currents calculated as the difference between the inward peak when stepping to 0mV and the steady state current before the end of the step (*dashed black lines* overlaid on *Fig. 4E*), N = 3 VTA microglia and N = 24 SNr microglia. **F-H** – Resting membrane potential (V_{rest}), membrane capacitance (C_m), and input resistance (Tau decay) of microglia are not correlated with time elapsed since acute brain slice preparation. Filled circles in a indicate cells from in which K_v currents were observed. **I** – Representative examples of microglia filled with biocytin via the recording pipette and stained for morphological analysis following recording. N = 4 - 5 biocytin-filled cells were examined per brain region and cells showed comparable levels of ramification.

Figure S3. Related to Figure 5.

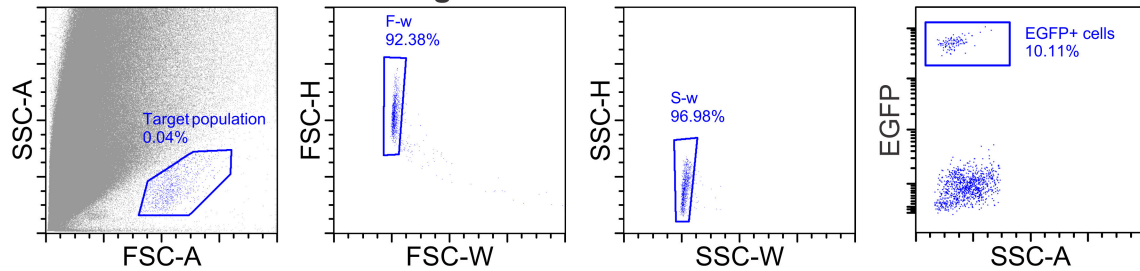
A Wildtype (EGFP-)



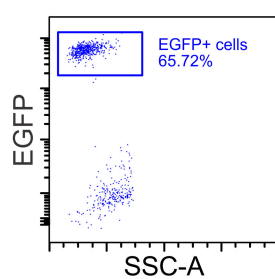
B Microdissected Cortex



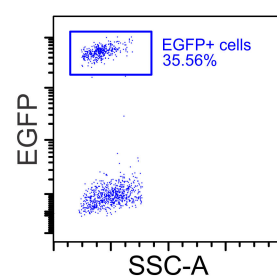
C Microdissected Ventral Tegmental Area



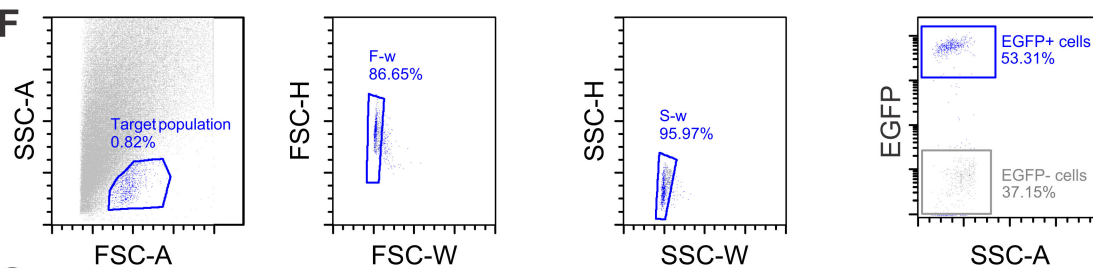
D Microdissected Nucleus Accumbens



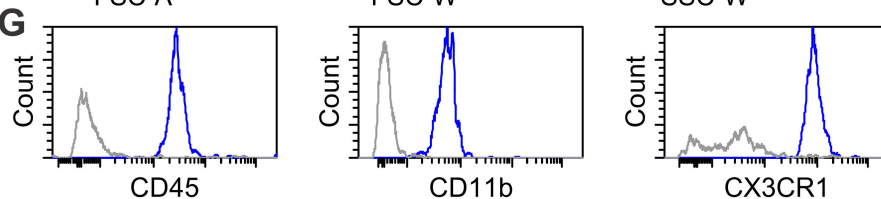
E Microdissected Substantia Nigra



F



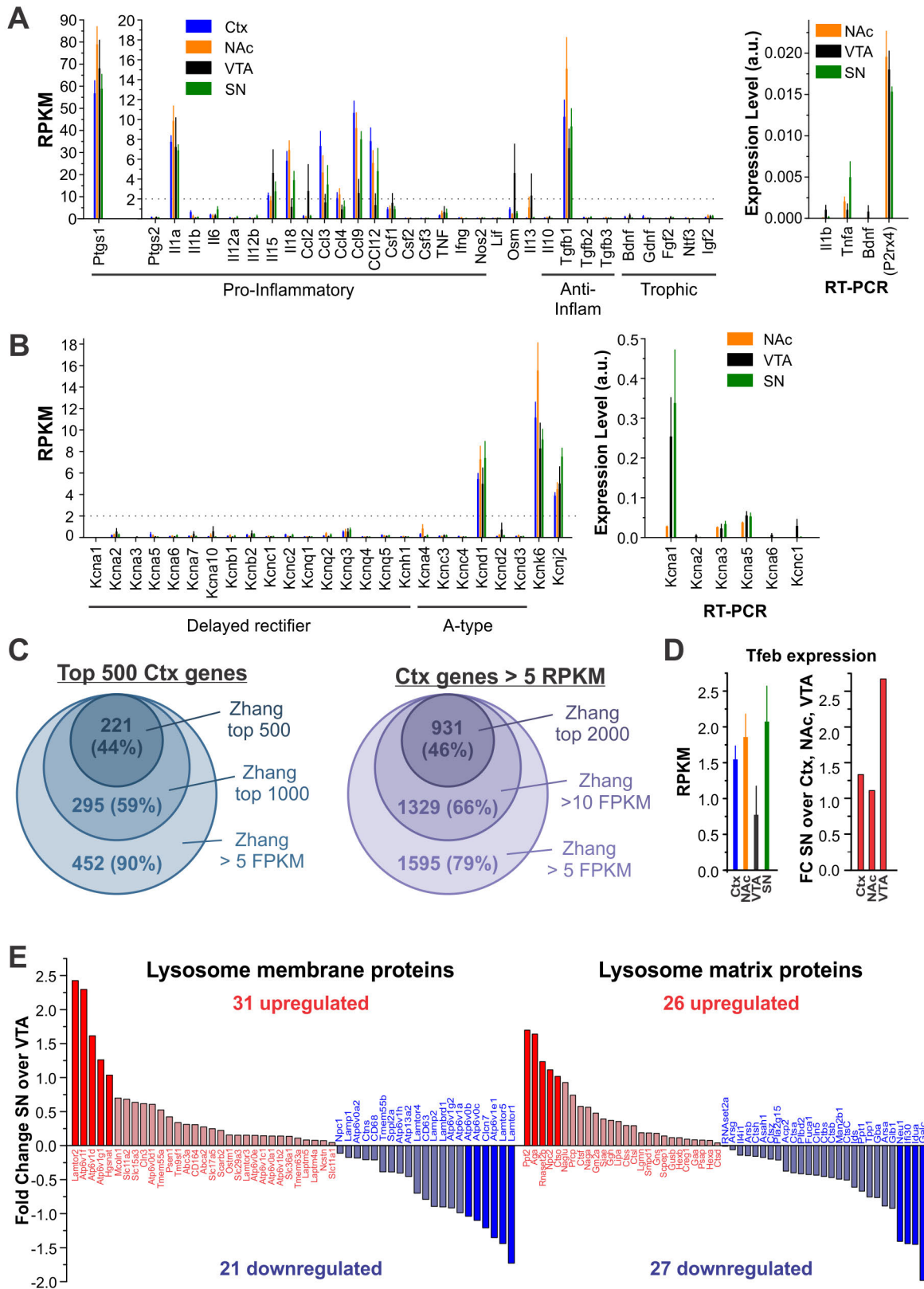
G



Supplementary Figure 3. Gating strategy for FACS-isolation of microglia. Related to Figure 5. A

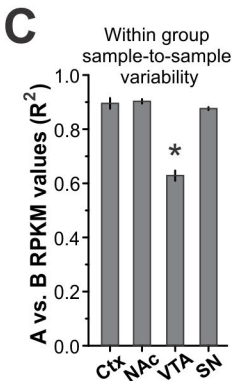
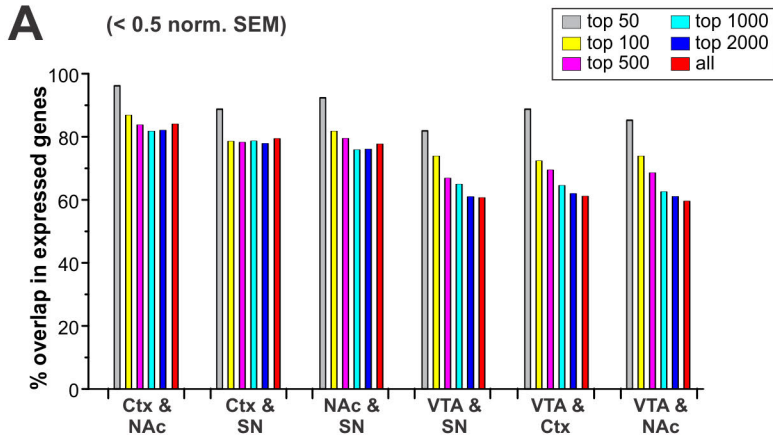
– Gating strategy applied to cortical tissue from a wildtype, C57Bl/6 mouse. *Left* – placement of gates for initial isolation of individual cells. Shown are side scatter (SSC-A, measure of cell granularity/complexity) and forward scatter (FSC-A, measure of cell size). *Middle* – placement of gates to refine collection of single cells using FSC height (H) and width (W) and SSC height and width. *Right* – placement of gates to separate EGFP⁺ and EGFP⁻ cells. No EGFP⁺ cells are present in wildtype, control tissue. **B-E** – Described gating strategy applied to microdissected tissue from cortex, nucleus accumbens, ventral tegmental area, and substantia nigra of a representative CX3CR1^{EGFP/+} mouse, showing robust separation between EGFP⁺ and EGFP⁻ cells. **F** – Isolation of individual EGFP⁺ cells (*blue points*) and EGFP⁻ cells (*gray points*) from cortical tissue from a CX3CR1^{EGFP/+} mouse following immunostaining. **G** – EGFP⁺ cells (*blue*) are immunopositive for CD45, CD11b, and CX3CR1, whereas EGFP⁻ cells (*gray*) are not.

Figure S4. Related to Figure 5.



Supplementary Figure 4. Validation of cell purity and gene expression patterns in RNAseq data. Related to Figure 5. **A** – Expression of inflammatory and trophic signaling factors within Ctx and BG microglia. *Left* – Inflammatory and trophic signaling factors commonly reported to be expressed or released by microglia as assessed by RNAseq. *Right* – expression of a subset of inflammatory and trophic factors as assessed by RT-PCR. Expression levels of *P2rx4* are shown for comparison to highlight that *I11b*, *Tnfa*, and *BDNF* expression is minimal. **B** – Expression of voltage-gated potassium channels within Ctx and BG microglia. *Left* – RNAseq analysis of delayed rectifier and A-type potassium channels most likely to underlie observed K_v currents (*Fig. 4B-F*). Also shown are *Kcnk6* and *Kcnj2*, which were the only additional potassium channels whose expression was detected within Ctx and BG microglia. *Right* – expression of a subset of delayed rectifier potassium channels as assessed by RT-PCR. N = 6 – 8 samples per group for all RNAseq data. All RT-PCR experiments were carried out on samples from an independent cohort of mice, N = 4 – 5 samples per region. *Gapdh* was used as an endogenous control for normalization and expression levels are expressed as $2^{-\Delta Ct}$ (a.u. = arbitrary units). **C** – Comparison of gene expression patterns in microdissected, FACS-isolated Ctx microglia and whole cortex microglia from Zhang et al. 2014. *Left* – number of genes and percentage overlap of our top 500 Ctx microglial genes (mean 63 ± 15 RPKM) with increasingly broad portions of the Zhang et al. cortex microglia dataset. *Right* – number of genes and percentage overlap of our Ctx microglial genes with RPKM > 5 and increasingly broad portions of the Zhang et al. cortex microglia dataset. **D** – Expression of transcription factor EB (*Tfeb*), master regulator of lysosome biogenesis. Data are shown as fold change in SN microglia over VTA, NAc, and Ctx microglia. **E** – Expression of lysosomal membrane and matrix proteins in SN as compared to VTA microglia. Genes exhibiting the largest fold changes are depicted in dark red or blue and names of the corresponding genes are listed.

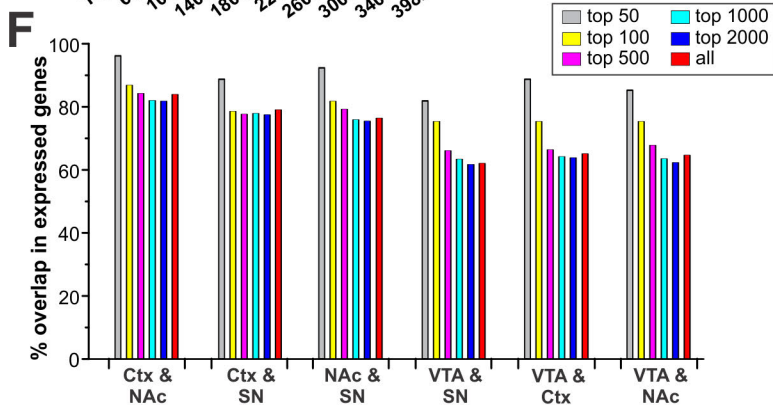
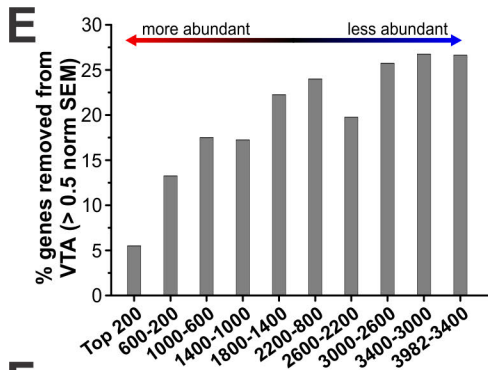
Figure S5. Related to Figure 6.



D

	# of genes			
	mean RPKM >2	norm SEM <0.5	removed	%removed
Ctx	4776	4767	9	0.19
NAc	5028	4999	29	0.58
VTA	3982	3150	832	20.89
SN	4164	4111	53	1.27

	# of genes			
	mn. RPKM >10	norm SEM <0.5	removed	%removed
Ctx	789	786	3	0.38
NAc	868	868	0	0
VTA	717	637	80	11.16
SN	620	618	2	0.32



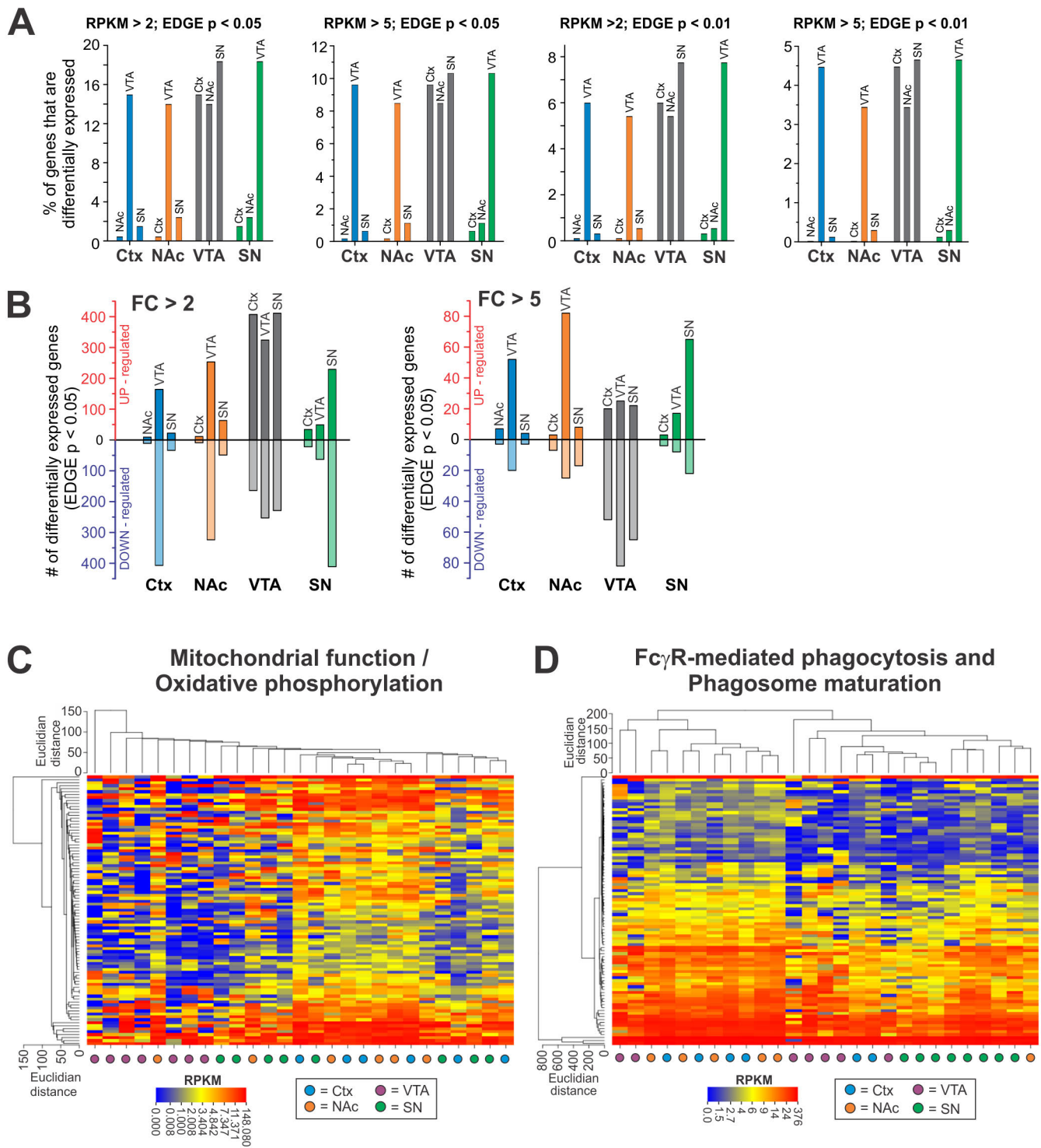
B

Top 50 enriched genes

Ctx	NAc	VTA	SN
Cst3	Cst3	Cst3	Cst3
Hexb	Malat1	Malat1	Malat1
Malat1	Hexb	mt-Co1	Hexb
mt-Co1	Ctsd	Hexb	mt-Co1
Ctsd	mt-Co1	Ctsd	Ctsd
B2m	C1qb	B2m	B2m
Ctss	B2m	Ctss	Ctss
C1qb	Ctss	C1qb	C1qb
mt-Cytb	mt-Nd1	mt-Nd1	mt-Cytb
Tyrobp	mt-Cytb	mt-Cytb	mt-Nd1
mt-Nd1	Tyrobp	Serinc3	mt-Nd4
mt-Nd4	Csf1r	Csf1r	Sparc
Serinc3	Serinc3	mt-Nd4	Serinc3
Csf1r	Sparc	Actb	Csf1r
Sparc	C1qc	Sparc	Tyrobp
Actb	mt-Nd4	P2ry12	mt-Co2
Tmsb4x	Actb	mt-Nd5	mt-Nd5
Lars2	Tmsb4x	mt-Atp6	C1qc
P2ry12	P2ry12	Tyrobp	mt-Atp6
mt-Co2	mt-Co2	C1qc	Actb
mt-Atp6	Lars2	Tmem119	Tmsb4x
C1qc	mt-Atp6	Tmsb4x	mt-Nd4l
mt-Nd5	mt-Nd4l	lvns1abp	Lars2
Fcrls	Selplg	mt-Co2	P2ry12
Itm2b	mt-Nd5	Selplg	Laptm5
Laptm5	Laptm5	Cd81	Selplg
Selplg	Fcrls	Laptm5	mt-Co3
mt-Nd4l	Fcer1g	Fcer1g	Cd81
Fcer1g	mt-Co3	Itm2b	Tmem119
Cd81	Tmem119	mt-Nd4l	lvns1abp
Fth1	C1qa	Ly86	Fcer1g
mt-Co3	Cd81	mt-Co3	Itm2b
Tmem119	Itm2b	Fth1	Ly86
C1qa	lvns1abp	Cx3cr1	Itgam
Sepp1	Sepp1	Itgam	Fth1
lvns1abp	Cx3cr1	C1qa	Cx3cr1
Calm2	Ly86	Mpeg1	C1qa
Ly86	Fth1	Epb4.112	Lgmn
Cd68	Lgmn	Sepp1	mt-Nd2
mt-Nd2	Calm2	Calm2	Fcrls
Cx3cr1	Cd68	Lgmn	Psap
Epb4.112	Itgam	Cd33	Sepp1
Lgmn	Epb4.112	Psap	Epb4.112
Itgam	mt-Nd2	Cd68	Ctsl
Tgfb1	Rps29	Rps29	Cd180
Sirpa	Sirpa	Lair1	Calm2
Mpeg1	Psap	Hsp90b1	Tgfb1
Rps29	Cd53	Fcrls	Hsp90b1
Cd53	Tgfb1	Tgfb1	Cd53
Psap	Ctsl	mt-Nd2	Sirpa

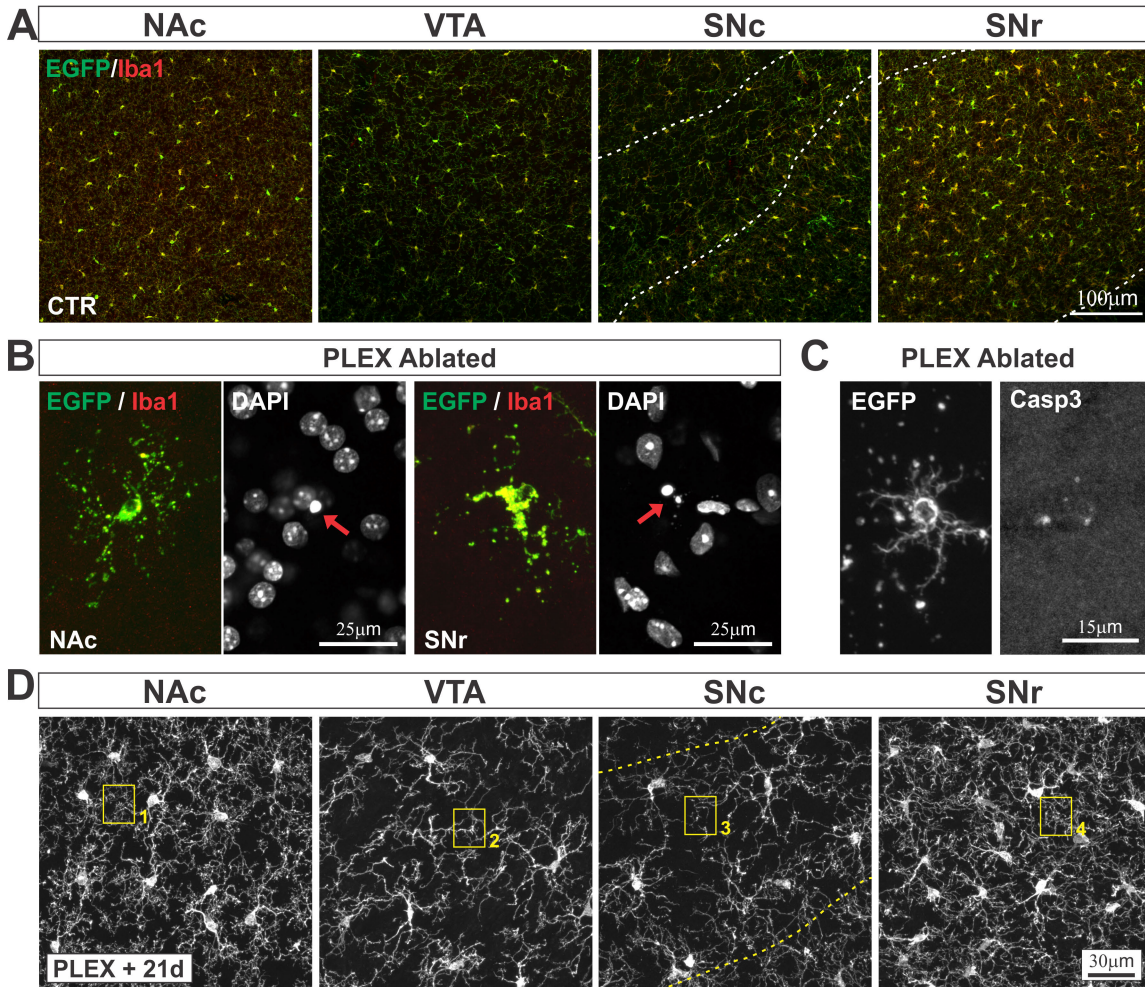
Supplementary Figure 5. Variation of analysis parameters does not influence general trends in differential gene expression. Related to Figure 6. **A** – Overlap in gene expression in pairwise comparisons of BG and Ctx microglia when restricting analyses to subsets of the most highly-expressed genes. In comparisons of “All” genes, equal numbers of genes in each region were compared, with the specific number of genes being determined by the region with a larger number of genes meeting threshold for expression (mean RPKM >2, norm SEM <0.5). For example, 4999 genes meet criteria for expression in NAc microglia and were compared to the top 4999 genes in VTA microglia. **B** – List of top 50 genes expressed in microglia from each region. Genes in *bold* are present in top 50 lists in all 4 regions. **C** – Sample-to-sample variability as measured by A vs. B comparisons of RPKM values; * $P < 0.0001$ all comparisons. **D** – Number and % of genes removed from analysis due to sample-to-sample variability. **E** – % of genes removed from analysis among more abundant and less abundant transcripts in VTA microglia; sample-to-sample variability is increased in lower abundance transcripts. **F** – Degree of overlap in expressed genes when filters for sample-to-sample variability (normalized SEM < 0.5) are removed; VTA microglia still displayed lower overlap in expressed genes compared to all other groups. In comparisons of “All” genes, equal numbers of genes in each region were compared, with the specific number of genes being determined by the region with a larger number of genes meeting threshold for expression (mean RPKM >2). For example, 5028 NAc microglial genes were compared to the top 5028 VTA microglial genes.

Figure S6. Related to Figure 6.



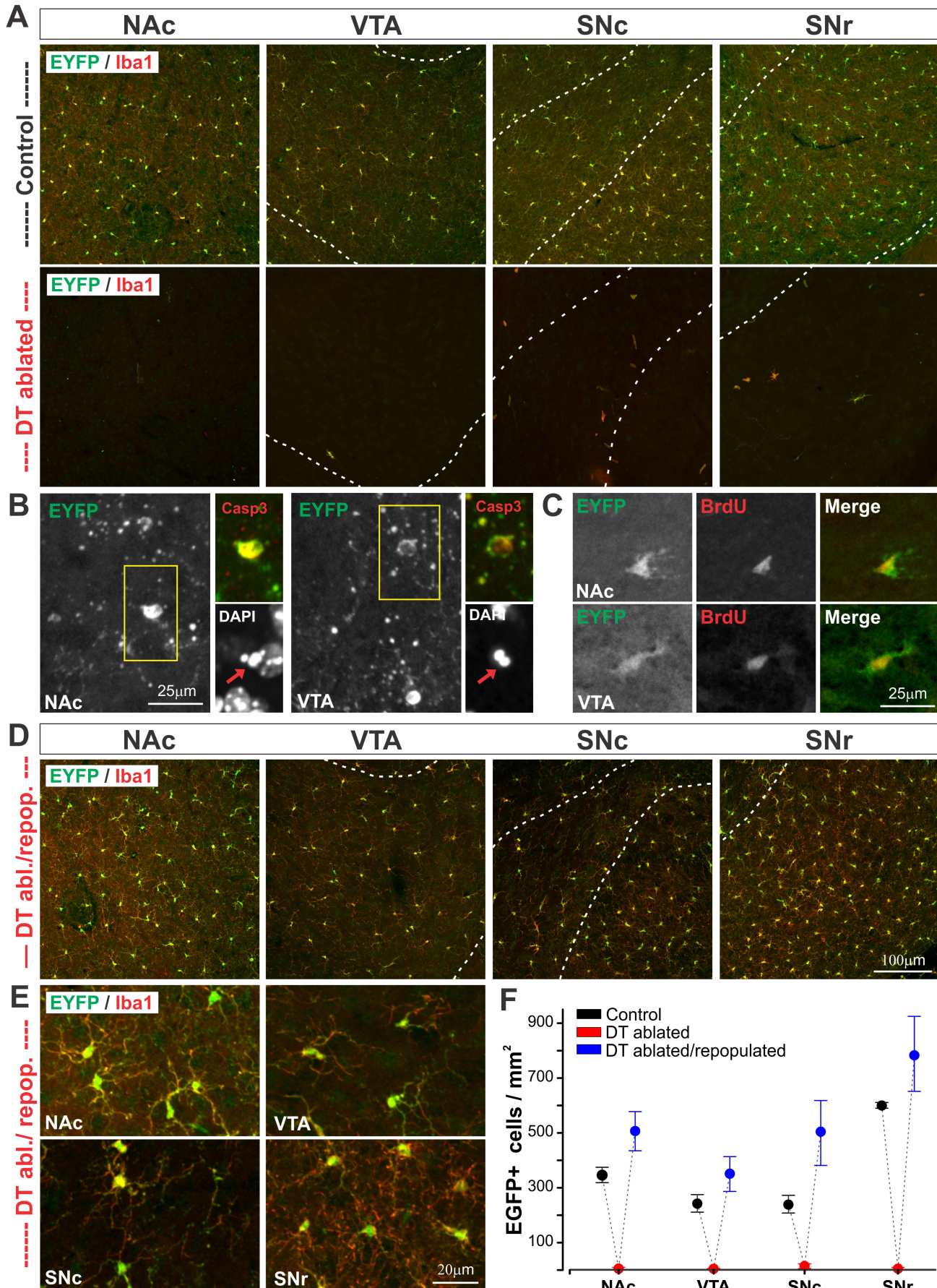
Supplementary Figure 6. Analysis parameters do not affect relative number of differentially expressed genes and differentially expressed VTA microglial genes are associated with multiple canonical signaling pathways. Related to Figure 6. **A** – Number of genes expressed at significantly different levels in pairwise comparisons of Ctx and BG microglia using EDGE test; numbers are displayed as a percentage of the total number of genes expressed by that pair of microglia. *From left to right* – similar analyses considering only genes with higher levels of expression (mean RPKM > 5) and using increasingly stringent *P*-value criteria ($P < 0.01$). **B** – Number of genes that are significantly up- or down-regulated in pairwise comparisons of Ctx and BG microglia using EDGE test ($P < 0.05$). All significantly up- and down-regulated genes are shown in *Figure 6B*. Significantly up- and down-regulated genes with fold change (FC) greater than 2 and greater than 5 are shown at *left* and *right*, respectively. **C** – Expression patterns for genes associated with Mitochondrial function and oxidative phosphorylation signaling pathways. Heat map shows RPKM values and unsupervised clustering of individual microglial samples on the basis of genes in this canonical signaling pathway. **D** – Expression patterns for genes associated with Fc γ receptor (Fc γ R)-mediated phagocytosis and phagosome maturation signaling pathways. Heat map shows RPKM values and unsupervised clustering of individual microglial samples on the basis of genes in this canonical signaling pathway.

Figure S7. Related to Figure 8.



Supplementary Figure 7. Treatment with CSF1R antagonist PLEX6552 for microglial ablation and repopulation. Related to Figure 8. **A** – Microglial distribution in BG nuclei in a $CX3CR1^{EGFP/+}$ mouse fed with control diet for a minimum of 14 days in parallel to mice being fed PLEX5622. Quantification of microglial cell density shown in Fig. 8E. *Dashed white lines* indicate the boundaries of the SNc and SNr. **B** – Additional examples of dying microglial cells from mice treated with PLEX5622 for 1 week (similar to Fig. 8B). Cells exhibit membrane blebbing and pyknotic nuclei (*red arrows*) characteristic of cells undergoing programmed cell death. **C** – Example of a microglial cell from a mouse treated with PLEX5622 for 1 week that exhibits both membrane blebbing and immunolabeling for cleaved caspase 3. **D** – Branching structure of microglia in PLEX ablated and repopulated mice. Regions highlighted by *yellow boxes* correspond to higher magnification images shown in Fig. 8D. Quantification of microglial tissue coverage shown in Fig. 8F.

Figure S8. Related to Figure 8.



Supplementary Figure 8. Genetic microglial ablation and repopulation. Related to Figure 8. A –

Distribution of microglia in BG nuclei of $CX3CR1^{Cre-ER-ires-EYFP/+};Rosa^{fs-DT/fs-DT}$ mice injected with vehicle (control, *top panel*) or 2 days after final injection of 4-hydroxytamoxifen (4HT, DT ablated, *bottom panel*). *Dashed white lines* indicate boundaries of VTA, SNc, and SNr. **B** – Examples of dying cells in brain sections from $CX3CR1^{Cre-ER-ires-EYFP/+};Rosa^{fs-DT/fs-DT}$ mice that were euthanized part way through the 4HT treatment (2 days of 4HT injections). Cells exhibit hallmarks of programmed cell death including: membrane blebbing, pyknotic nuclei (*red arrows*), and immunoreactivity for cleaved caspase 3 (*Casp3*). **C** – Examples of proliferating 5-bromo-2-deoxyuridine (BrdU)+ cells observed during repopulation; $CX3CR1^{Cre-ER-ires-EYFP/+};Rosa^{fs-DT/fs-DT}$ mice were treated with 4HT and then injected with BrdU for 2 days before being euthanized. % of EYFP+ cells that were BrdU+, NAc $76 \pm 5\%$, VTA $48 \pm 4\%$, SNr $74 \pm 7\%$. **D** – 4HT-treated mice at 6 weeks post final 4HT injection (DT ablated/repopulated). **E** – High magnification images showing branching structure of BG microglia in DT ablated/repopulated mice. **F** – Quantification of microglial cell density in control, DT ablated, and DA ablated/repopulated mice. For DT ablated/repopulated mice, microglial cell density values were normalized to a BG-wide density average for each mouse to obtain normalized values shown in *Figure 8G*.

Table S4. Primers and probes used for RT-PCR experiments. Related to Figures 5 and S4.

Gene	TaqMan Assay ID or custom probe	Forward primer	Reverse Primer
<i>P2rx1</i>	Mm00435460_m1		
<i>P2rx4</i>	Mm00501787_m1		
<i>P2rx7</i>	Mm01199500_m1		
<i>P2ry1</i>	Mm00435471_m1		
<i>P2ry2</i>	Mm04207602_m1		
<i>P2ry6</i>	Mm01275472_m1		
<i>P2ry12</i>	Mm00446026_m1		
<i>Il1b</i>	Mm00434228_m1		
<i>Tnf</i>	Mm00443258_m1		
<i>Bdnf</i>	Mm01334042_m1		
<i>Kcna1</i>	FAM-AAAGTGATACGAGGGTAGAAA-MGB	TGGACGGCTGCAGAGAAATA	GTCGTCCCATCAGAATGCT
<i>Kcna2</i>	Mm01197194_m1		
<i>Kcna3</i>	Mm00434599_s1		
<i>Kcna5</i>	Mm00524346_s1		
<i>Kcna6</i>	FAM-CTGCACGAGGCCAC-MGB	CTTTCTTGCCTCTGAGGGTTGT	TCTTTGGATGCATAGGTTTTCCA
<i>Kcnc1</i>	Mm00657708_m1		
<i>Gapdh</i>	MGB - CTCATGACCACAGTCCA - VIC	GACAACTTTGGCATTGTGGAA	CACAGTCTTCTGGGTGGCAGTGA